Monte Carlo Simulation of Spacecraft Particle Detectors to Assess the True Human Risk

P.M. O'Neill
NASA Johnson Space Center, Houston, Texas 77058-3696

Abstract

Particle detectors (DOSTEL, CPDS, and TEPC) measure the energy deposition spectrum inside earth orbiting - manned spacecraft (shuttle, space station). These instruments attempt to emulate the deposition of energy in human tissue to evaluate the health risk. However, the measurements are often difficult to relate to tissue equivalent because nuclear fragmentation (internuclear cascade / evaporation), energy-loss straggling, heavy ions, spacecraft shielding and detector geometry/orientation, and coincidence thresholds significantly affect the measured spectrum. We have developed a high fidelity Monte Carlo model addressing each of these effects that significantly improves interpretation of these instruments and the resulting assessment of radiation risk to humans.

1.0 Introduction

Particle detectors such as the two-element telescope DOSTEL [1], the Charged Particle Detector System (CPDS) [2], and the Tissue Equivalent Proportional Counter (TEPC) [3, 4] measure the energy deposition spectrum inside earth orbiting - manned spacecraft such as shuttle, space station, and Mir. These measurements are necessary to access the risk to humans and to micro-electronic components – computer chips. Of course analytical models which include simple transport codes, such as CREME96 and HIZ [5-7], are available for computing the ionizing radiation environment inside these spacecraft. However, verification and revision of these models is an ongoing effort that requires in-situ measurement.

For example, high LET particles and even neutron fluxes produced by interaction of the space environment with spacecraft shielding could be especially harmful (to humans and chips) and may not always be faithfully rendered by simple radiation models.

On the other hand, instrument measurements are difficult to interpret because of interactions of the radiation environment with the instrument itself. Nuclear fragmentation within the detector must be discerned from secondary particles produced within the spacecraft walls. Energy-loss straggling caused by dispersions in the electron – ion interactions as the ion traverses the thin silicon detector tends to broaden the measured spectrum. Detector geometry and orientation within the spacecraft, and coincidence thresholds are also important considerations.

The aid of analytical models to access the impact of each of these effects is considered in the following paragraphs for the two-element DOSTEL instrument.

2.0 DOSTEL

The DOSTEL has two 315 micron thick, 27 mm diameter silicon detectors spaced 15 mm apart as shown in Figure 1. DOSTEL flew inside the Shuttle on flight STS-84 (May 15-24, 1997) at an orbital altitude of 210 nautical miles in a 51.6 degree inclination orbit. The DOSTEL was placed in the Orbiter where the shielding is known to be approximately 1" aluminum toward the front and 4" to the rear [8]. The shielding assumed here is 1", 2", 3", and 4" for equal solid angle segments from 0 to 60, 60 to 90, 90 to 120, and 120 to 180 degrees respectively. This approximation reasonably accounts for increasing wall thickness toward the rear of DOSTEL.

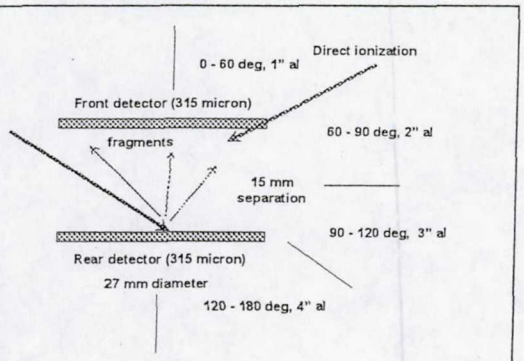

Figure 1 DOSTEL (2-element particle detector) geometry and orientation relative to orbiter shielding approximation

The instrument measures the energy deposited in the front detector. However, particles are counted when a coincidental energy deposition of >64 KeV occurs in each detector. The instrument does not record the count unless the count rate exceeds 50 per second. This restricts data acquisition to the heart of the South Atlantic Anomaly (SAA) where the proton flux is sufficient. The DOSTEL recording ground track for STS-84 SAA passes is shown in Figure 2.

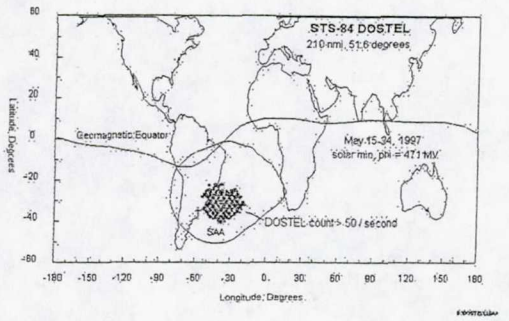

Figure 2 For STS-84 DOSTEL recorded flux in the heart of the SAA

Particles can enter DOSTEL from the front, the rear, or the side. However, direct ionization particles that pass straight through each detector must enter the front or rear at an angle from 0 to 60 degrees from the normal in order to hit both detectors coincidentally. However, particles entering the sides can interact in one of the silicon detectors and produce fragments which may produce coincidence.

The LET (Linear Energy Transfer) in silicon (measured by DOSTEL) is determined by the energy deposited in the front detector and the effective thickness of the detector (assuming that all of the direct ionization protons arrive at the mean angle 34 degrees):

LET(si, DOSTEL, MeV cm**2/g) = ΔE(MeV)/(t(g/cm**2)secant(34 deg))

The LET in tissue (measured by DOSTEL) is found by first multiplying the LET in silicon (MeV cm**2 /g) by 1.31 (the assumed ratio of energy loss in tissue to energy loss in silicon per unit mass for 100 MeV protons) to get the

LET in tissue in MeV cm**2/g and then converting this to KeV / micron tissue by dividing by ten since the density of tissue is assumed to be 1 g / cm**3. Therefore,

LET(tissue,DOSTEL,KeV/micron) = 0.131*LET(si,DOSTEL,MeVcm**2/g)

3.0 Monte Carlo Model Description

Figure 3 shows the actual DOSTEL measurements and a simplified model calculation of the tissue LET spectrum for the SAA passes of STS-84. Here, the simplest model is assumed where only the contribution of direct ionization protons is considered– showing that direct ionization does not account for the low and high ends of the LET spectrum.

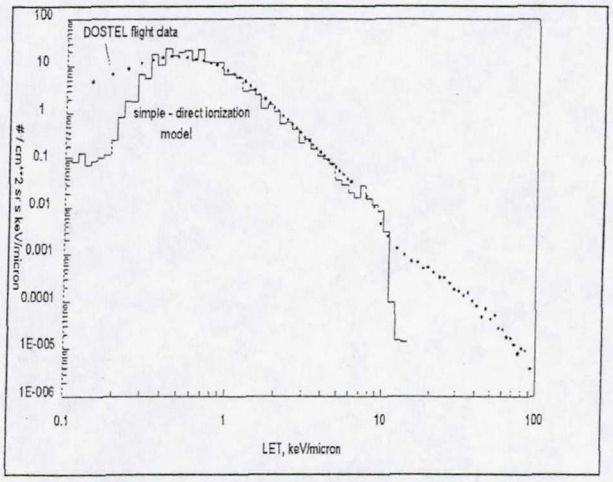

Figure 3 Actual DOSTEL measurement and direct ionization model of tissue LET spectrum

To refine the model to include more subtle effects, DOSTEL is modeled with a Monte Carlo simulation that emulates the actual instrument identically. The effects of nuclear fragmentation, energy-loss straggling, Galactic Cosmic Rays (GCR), albedo protons, spacecraft shielding, detector geometry / orientation and coincidence thresholds are considered.

The trapped plus GCR proton flux outside the Orbiter is calculated as the Orbiter moves in earth orbit. This proton flux is calculated every 30 seconds along the trajectory using AP8MIN [9] for trapped protons and HIZ [5-7] for GCR's. The AP8MIN model uses the IGRF 64/65 geomagnetic field [10] and the HIZ model used the solar modulation deceleration parameter of 471 MV which was determined from the Climax neutron count corresponding to the STS-84 flight time. This flux is propagated through the Orbiter shielding and the number of protons from the front segment (0 to 60 degrees) plus the rear segment (120 to 180 degrees) is monitored. When the integral flux above 7 MeV exceeds 50 per second, the simulated DOSTEL starts to track protons in the detectors as described below. Note that 7 MeV is required to pass one of the 315 micron detectors at 34 degrees with 64 KeV remaining. The model, just like the actual instrument, records the energy deposited in the front detector when a coincidental energy deposition of >64 KeV occurs in each detector. Protons from the side segments (60 to 120 degrees) are negligible because they cannot hit both detectors to produce coincidence by direct ionization (only by fragmenting).

When the simulated DOSTEL count rate exceeds 50 per second, the proton energy, direction, and point of impact on the DOSTEL is chosen statistically in Monte Carlo fashion. Particles that enter DOSTEL from the front, the rear, or the side are propagated in a detector (if they hit one) until they exit, stop, or cannot hit the other detector.

Most of the protons deposit energy by direct ionization. However, the

accumulated track length is monitored and based on the mean free path in silicon, a nuclear interaction occurs when the likelihood of an event is statistically exceeded in Monte Carlo fashion. When a proton - silicon interaction occurs, fragments are produced that generally contribute to energy deposition. The nuclear interaction code CLUST-EVAP [8] is used to determine the composition of particle fragments and each of their energies and directions. The direct ionization path and deposition of each of these fragments is then tracked in the detectors as for protons.

4.0 Model Applications

In the first approximation, the DOSTEL LET spectrum can be accounted for by simply assuming only direct ionization by trapped protons as in Figure 2. Here, the AP8MIN model has been extrapolated to 2 GeV with power law, otherwise, no protons above 500 MeV are included in AP8MIN.

The model is in excellent agreement with the measurement over a large range, except at low (< 0.3 KeV / micron) and high (> 10 KeV / micron) LET. This is especially important because there were absolutely no arbitrary adjustments made in the model's flux magnitude. This suggests that the Orbiter shielding assumed (1", 2", 3", and 4") is reasonably correct and that the AP8MIN spectrum has the correct shape and magnitude.

We now investigate the various radiation effects, which could possibly contribute to the measured flux.

4.1 Straggling

The energy loss has a probability distribution that is described by the Vavilov function [11]. For thin detectors, the delta ray electrons can have sufficient energy to escape from the detector. This leads to smaller energy loss and less energy loss fluctuations. Badhwar [12] developed a modification to the Vavilov distribution to allow for electron escape. The particle path length in the detector and hence the electron energy required to escape is a function of angle. The modified theory was used to determine the energy loss in the detector and took this into account.

Figure 4 shows that this effect increases the flux below LET's of 0.3 KeV/micron but that straggling does not account for all the disagreement in this region.

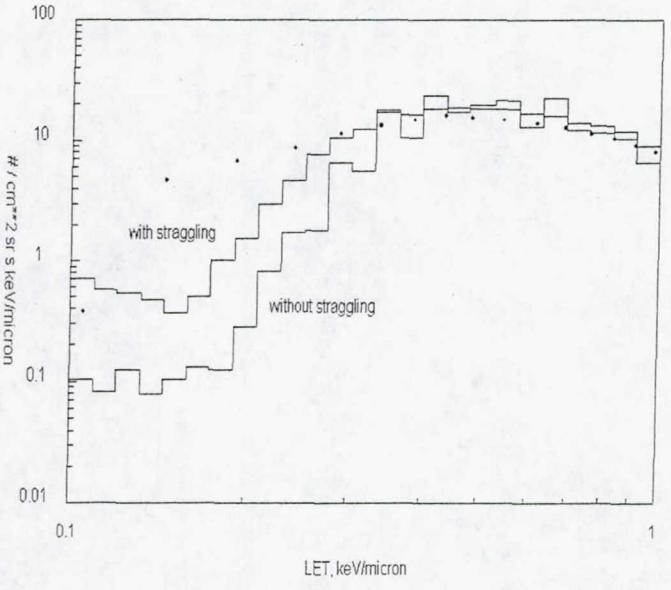

Figure 4 LET spectrum at low LET shows that accounting for straggling improves agreement with DOSTEL measurement, but does not entirely explain the discrepancy

4.2 Fragments

The proton-induced target spallation is modeled as a two-step process, the cascade and evaporation stage. In the cascade stage, the proton, on entering the nucleus, collides with another nucleon, and this in turn collides with other nucleons. Some nucleons are ejected from the nucleus, which is left in an excited state. The excitation energy is shared by the nucleons, with the system characterized by "nuclear temperature". In the evaporation stage, the nucleons boil off isotropically in the rest frame of the nucleus. O'Neill et al. [17] combined the work of Mathews et al. [14] and Tang et al. [15] to develop the intranuclear- evaporation model. Figure 5 shows the model contribution to the actual DOSTEL LET spectrum due to fragments. This is clearly a significant contribution for LET > 10 KeV / micron and accounts for practically all the flux in this region.

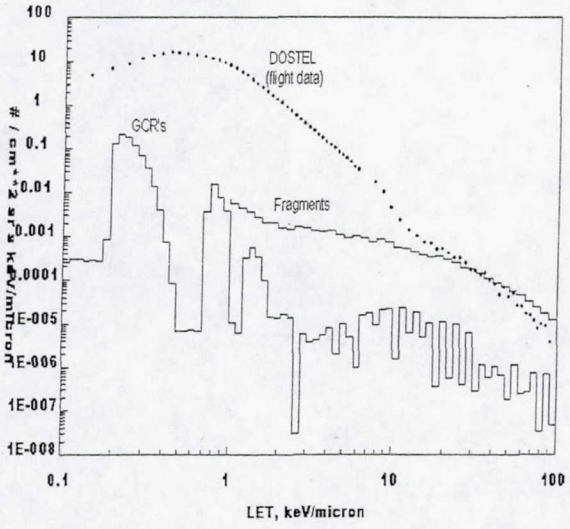

Figure 5 LET spectrum shows that nuclear fragments from protons interacting with the silicon detectors is much more significant than GCR's – up to 100 kev/micron tissue.

4.3 Additional Contributions

The Galactic Cosmic Ray (GCR) contribution (while within the SAA when the DOSTEL threshold is exceeded) to the flux in Figure 5 shows that below 100 KeV / micron the GCR component accounts for very little of the flux. One might suspect that at low LET's, the GCR proton component could make a significant contribution, but this is clearly not the case. Also, in the region from 10 – 100 KeV / micron, the contribution from fragments over shadows that from GCR's. The only region where GCR's could possibly contribute are beyond the DOSTEL limit of 100 KeV / micron.

In addition to the trapped protons, there are albedo protons present. The albedo proton spectrum was measured on the June 1998 STS-91 (51.65' x 380 km), close to the time of the last solar minimum. This spectrum extends from 70 MeV to 12 GeV [16]. The spectrum was extended to energies lower than 70 MeV using the expression of Armstrong and Colburn [17] normalized at 70 MeV. This albedo contribution is shown to be insignificant [8].

5.0 Conclusion

Figure 6 shows the complete DOSTEL spectrum – actual and model. The excellent agreement clearly demonstrates the fidelity of the model. Only at very low LET (< 0.25 KeV/micron) is there significant difference. In this region, various contributing suspicious sources have been eliminated – GCR's, albedo, straggling – all have been acquitted.

The significance of the model – actual agreement is a good indication that the existing transport models are reasonably accurate.

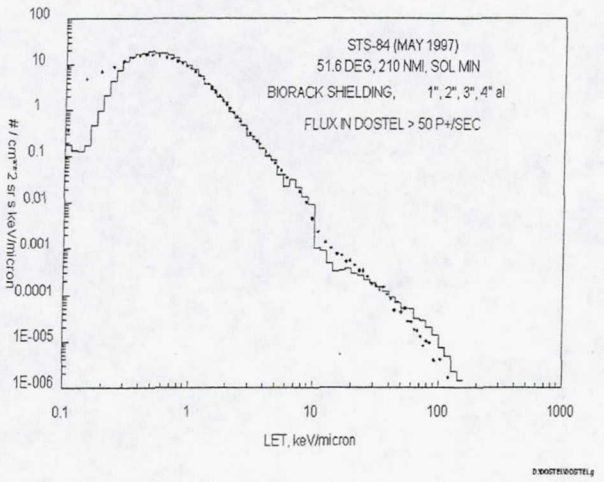

Figure 6 DOSTEL and high fidelity Monte Carlo model LET spectra

5.0 References

[1] R. Beaujean, J., Kopp, G. Reitz, Radiat. Prot. Dosim. 85 (1-4) (1999) 223.

[2] G.D. Badhwar, W. Atwell, E.V. Benton, A.L. Frank, R.P. Keegan, V.E. Dudkin, O.N. Karpov, Yu.V. Potapov, A.B. Akopva, N.V. Magradze, L.V. Melkumyan, Sh.B. Rshtuni, Radiat. Meas. 24 (1995) 283.

[3] G.D. Badhwar, F.A. Cucinotta, L.A. Braby, A. Konradi, Radiat. Res. 139 (1994) 344.

[4] G.D. Badhwar, A. Kohradi, W. Atwell, M.J. Golightly, F.A. Cucinotta, J.W. Wilson, V.M. Petrov, I.V. Tchernykh, V.A. Shurshakov, A.P. Lobakov, Radiat. Meas. 26 (2) (1996) 147.

[5] Adams J. H., Jr. Silberberg R. aud Tsao C. H. (1986) Cosmic Ray Effects on Micro Electronics, Part IV. Naval Research Laboratory Memorandum Report 5901, December 1986.

[6] Badhwar G. D. and O'Neill P. M. (1996) Galactic cosmic radiation model and its applications. Adv. Space Res. 17, 7-17.

[7] Badhwar G. D. and O'Neill P. M. (1993) Tiine lag of twenty-two year solar modulation. In Proc. 23rd Int Cosmic Ray Conf. 3, pp. 535-539.

[8] Badhwar G. D. and O'Neill P. M. (1996) Response of silicon-based linear energy transfer spectrometers: implication for radiation risk assessment in space flights. Nucl. Instr. & Meth. A 466 (2001) 464-474.

[9] D.M. Sawyer, J.E. Vette, AP8 trapped proton environment for solar maximum and solar minimum, Report NSSDC/NVDC-A-R&S 76-06, NASA Goddard Space Flight Center, Greenbelt, MD, 1976.

[10] International Geomagnetic Field 1965, J. Geophys. Res. 74 (1969) 4407.

[11] P.V. Vavilov, Zh. Theor. Fiz 32 (1957) 320; JETP 5 (1957) 749.

[12] G.D. Badhwar, Nucl. Instr. and Meth. A 109 (1973) 119.

[13] P.M. O'Neill, G.D. Badhwar, W.X. Culpepper, IEEE Trans. Nucl. Sci. NS-45 (6) (1998) 2467.

[14] G.J. Mathews, B.G. Glagola, R.A. Moyle, V.E. Viola Jr., Phys. Rev. 25 (1992) 2181.

[15] H.H.K. Tang, G.R. Srinivasan, N. Azziz, Phys. Rev. 42 (1990) 1598.

[16] G.D. Badhwar, A.G. Troung, P.M. O'Neill, V. Choutko, Radiat. Meas. 3(3) (2001).

[17] T.W. Armstrong, B.L. Colburn, Nucl. Tracks Radiat. Meas. 20 (1992) 101.